Predicting the activity of protein-ligand complexes

Lukas Fallmann

BACHELORARBEIT

eingereicht am

Fachhochschul-Bachelorstudiengang

Medizin- und Bioinformatik

in Hagenberg

im Juni 2023

Advisor:

Micha Johannes Birklbauer, M.Sc.

Declaration

I hereby declare and confirm that this thesis is entirely the result of my own original work. Where other sources of information have been used, they have been indicated as such and properly acknowledged. I further declare that this or similar work has not been submitted for credit elsewhere. This printed copy is identical to the submitted electronic version.

Hagenberg, June 27, 2023

Lukas Fallmann

Contents

Preface

Abstract

This should be a 1-page (maximum) summary of your work in English.

Kurzfassung

An dieser Stelle steht eine Zusammenfassung der Arbeit, Umfang max. 1 Seite. ...

Acronyms

ACC Accuracy. 8, 12
AcH Acetylcholine. 4
AChE Acetylcholinesterase. vi, 4, 12
AUC Area under the curve. 8

COX1 Cyclooxygenase 1. 4
COX2 Cyclooxygenase 2. 4

DPP4 Dipeptidyl peptidase IV. 4

EF enrichment factor. 8

FPR False positive Rate. 8

HTS High-throughput screening. 1

KNN K nearest neighbor. 13

LBVS ligand basedvirtual screening. 1

MAOB Monoamine oxidase B. 5
MDI Mean Decrease in Impurity. 9

PCA Principal component analysis. vi, 11
PLIP protein ligand interaction profiler. 2

REF relative enrichment factor. 9

SMOTE Synthetic Minority Over-sampling Technique. 11, 12, 14
SVD singular value decomposition. 11

VS virtual screening. 1

Ya Yield of actives. 8

Chapter 1

Introduction

The discovery of new drugs or any chemically active compounds for that matter is an expensive and time-consuming process. It has been estimated, that it takes about 14 Years from the initial discovery of a promising new compound to the release of a marketable drug[1]. In addition to that the price of this drug-discovery circle ranges up to 800 Million Dollars[2]. All techniques which aim to improve the efficiency of drug discovery can generally be categorized as one of two methods. These two are called High-throughput screening (HTS) and virtual screening (VS)[1].
When using an HTS-approach there are many compounds which are tested against some type of target protein. Target proteins are usually proteins which are of general interest for medical use. During testing, it is measured whether a certain compound biochemically interacts with a protein. Those interacting combinations are considered active and are marked by researchers as hits. To improve the performance of HTS there are a number of factors to consider. Through miniaturization, it is possible to investigate more compounds at the same time. With a higher throughput quality-control is more time-consuming and leads to an overall more expensive process. For this reason HTS is most efficient, when analyzing a small set of compounds as the technology is not suitable for large datasets[3].
In contrast to the in vitro approach of HTS, VS is a theoretical in silico approach. To save resources in the laboratory the activity of certain compounds is predicted using a preexisting library of small molecules. The activity can be predicted using the ligands of a compound and their respective binding sites or the 3D structure of a compound. The Key idea behind the ligand based approach (LBVS) is that similar compounds have similar chemical properties. Therefore, the goal of LBVS is to find molecules which have similar or identical chemical properties as the sample compound[4]. Structure-based VS uses the 3D structure of a compound to predict which molecules from the dataset will bind to the provided sample. Each molecule of a certain database subset is fitted (docked) to the sample. Hereby it is important to differentiate between rigid and flexible docking[5].
In rigid docking the dataset sample is rotated and translated in a six-dimensional space in order to fit the sample protein. For each fitted molecule a score is calculated based on how well the molecule fits to the sample[6]. Although this algorithm often predicts actual possible binding sites and bound proteins, there is no guarantee that this compound will actually bind in vitro. Therefore, predicted interactions should be seen as a hypothesis.

Still rigid docking provides a great baseline at a comparatively low cost[4]. The low accuracy of rigid docking is due to the nature of biochemical substances as samples in a database can only provide a snapshot of a sample[5]. With flexible docking it is possible to simulate moving binding sites, where the flexibility can be introduced at different stages. Implicit flexibility is achieved by smoothing protein surfaces and therefore allowing room for interpretation when docking. Cross- or Ensemble docking can be done by repeating the docking process with different conformation and explicit flexibility is reached through allowing side-chain flexibility. Most commonly utilized is the approach where the ligand is flexible, and the receptor is rigid. Even though this approach does provide better more accurate results it takes considerably longer to compute[5].
Regardless of the docking type the score should reflect which pose between a protein and a ligand is most likely to exist. In addition to that, the score also determines whether a protein-ligand complex is considered active. There are a lot of different scoring functions which can be grouped into four categories: physics-based, empirical, knowledge-based, and machine learning-based[7].
The focus of this work is on implementing a machine-learning based scoring approach. Machine-learning based scoring functions work by training on labeled data and finding the best model for predicting future data. To accurately and efficiently train a model crucial binding sites need to be identified beforehand. The basis of this thesis is the master thesis of Birklbauer Micha[8]. In his thesis a selection of eleven proteins from the directory of useful decoys[9] have been selected to be analyzed. For the selected proteins all possible interactions have been analyzed by *PLIP*, which is an algorithm designed to discover various interactions based on the physical properties of a compound[10]. Based on the interaction-data a few basic scoring functions have been implemented. The direct result of this thesis are proteins and the frequency of their interactions.
Since this work aims to implement different machine learning algorithms for use in drug discovery the state of the art is described in the following.

1.1 Machine Learning in drug design and activity prediction

The following chapter summarizes the recent developments in drug design using various machine learning techniques.

Today there exist a multitude of machine learning approaches in the field of drug design and activity prediction. As a result of various AI breakthroughs in recent years there have been numerous research projects regarding the usability of artificial intelligence in various bioinformatic domains. One area where machine learning can be applied is quality assessment. *SVMQA* utilizes support vector machines to assess the quality of structural protein models[11]. Support Vector machines have also been used for the *DeNovo* algorithm to detect protein-protein interactions[12]. AI has also been used to successfully identify drug responsive biomarkers in pre-clinical data using regression algorithms[13]. In the field of synthesis-prediction AI has largely replaced the rule- and heuristic-based systems in place since the 1960s[14].

Due to developments in the field of deep learning, this technology has found numerous applications in biochemistry[15]. One of which is *deepDTnet*, which is a deep learning based algorithm used to identify new targets and repurpose existing drugs in a drug-gene-disease environment. This is done by embedding already existing interaction profiles into low dimensional vector spaces[16]. Deep learning also has its applications in the classification and segmentation of microscopic imagery[17]. *MILCDock* uses the Output of five traditional Scoring Functions as input for a neural Network. The input for the neural network comes from the tools *LeDock*, *Autodock Vina*, *PLANTS*, *Autodock4*, and *rDock*. This technique has a slight performance benefit when compared to traditional scoring functions [18].

1.2 Goals

The goals of this thesis are twofold:

1. Evaluate common machine learning approaches for activity prediction and compare results with current literature.
2. Evaluate the results posed by various feature engineering techniques and investigate the possible performance benefits for the implemented ML approaches.

The second goal can be viewed as an extension of the first one since its primary aim is to improve the results achieved while pursuing the first goal.

Chapter 2

Methods

2.1 Data description

The following chapter is dedicated to explaining the data used for this thesis. This includes detailed descriptions of the protein complexes as well as their interaction types.

2.1.1 Proteins

The following five proteins have been used as grounds for this thesis:

Acetylcholinesterase

Acetylcholinesterase (AChE) is an enzyme in the nervous system that breaks down Acetylcholine (AcH), a messaging molecule, into choline and acetate. It's found in high concentrations at junctions between nerve cells and muscles. AChE has various functions beyond just breaking down Ach, and it's present in both nerve and non-nerve tissues. Because AChE is so important, some toxins like insecticides and nerve agents target it. This versatility of AChE makes it a key player in nervous system function and a potential target for drugs to treat diseases[19].

Cyclooxygenase 1

Cyclooxygenase 1 (COX1) and its isoform Cyclooxygenase 2 (COX2) play a substantial role in synthesising various prostaglandins. Due to their linkage with inflammations and pain COX molecules are often targeted by anti-inflammatory drugs. In contrast to COX2, COX1 is found in most tissues across the body. In addition to that COX1 is largely attributed with homeostatic functions such as hemostasis and gastric cytoprotection[20].

Dipeptidyl peptidase IV

Dipeptidyl peptidase IV (DPP4) protein is partially responsible for hydrolysis of a prolyl bond between two residues from the N-terminus. DPP4 is present in several processes including metabolism and cancer biology. Due to its role within metabolism DPP4 inhibitory drugs have been successfully used in the treatment of diabetes type two.

DPP4 also plays a substantial role in the diagnosis of certain types of cancer. In most cases DPP4 is up regulated near cancerous growth, therefore locally elevated DPP4 levels can be an indicator for cancer[21].

Monoamine oxidase B

Monoamine oxidase B (MAOB) plays a major role in the breakdown of neurotransmitters (monoamines) within the body. The compound is mainly expressed in glial-cells and platelets. Its function categorizes MAOB as an important research compound, as MAOB inhibition has been proven to improve various neurological conditions. This stems from the fact that changes in the monoamine levels are associated with a myriad of neurological problems[22].

Soluble epoxide hydrolase

Soluble epoxide hydrolase (sEH) is part of an inflammatory pathway similar to COX. It has been shown that inhibition of sEH reduces inflammation. In contrast to COX it does not completely disable the synthesis of pro-inflammatory compounds but rather balance their levels[23].

2.1.2 Interactions

Interactions define how proteins interact with each other or other types of ligands. There are a lot of interactions which can be used for determining whether a certain compound might be considered active. The following interactions have been used by the PLIP-Algorithm to produce the base data for this thesis:

interaction	description[8]
hydrogen bonds	A hydrogen bond is defined as the interaction between a hydrogen atom, connected to a more electronegative atom, and another atom or molecule.
water bridges	A water bridge occurs when the ligand and the protein both bind to a water molecule through hydrogen bonds.
salt bridges	Salt bridges are ion pairs which stick together due to large difference in charge and the resulting electrostatic interaction.
halogen bonds	Halogen bonds are defined as the interactions between the electrophilic region around a halogen atom and a nucleophilic region.
hydrophobic interactions	Aggregates formed as a result of a hydrophobic interaction between hydrocarbons in an aqueous medium are called hydrophobic interactions.
pi-stacking	Interactions between neighboring aromatic rings are called pi-stacking. Due to the pi-electron density the ring is partially positively charged around the periphery and negatively charged above both aromatic faces. As a result electrostatic forces build between aromatic rings, and they are attracted to one another.
pi-cation	Cations and pi-stacks who bind through electrostatic forces at a pi-stacks face are called pi-cation interactions.

Table 2.1: interaction types

2.1.3 Data origin and structure

The provided data is a byproduct of the thesis [8] by Micha Birklbauer. The interaction data was produced using the *PLIP Algorithm* [10] on the aforementioned proteins.

The PLIP Algorithm consists of four major stages:

Structural Preparation – SP
: During the preparation step the input structure is hydrogenated and the ligands(including their binding sites) are extracted.

Functional Characterization – FC
: Using the structure of the complex a myriad of functional groups are detected. This includes binding site atoms, hydrophobic atoms and aromatic rings just to name a few.

Rule Based Matching – RBM
: In the third step the algorithm investigates all interactions between the ligand and the protein, which can be attributed to geometric constraints. Hydrogen bonds are detected here.

Filtering of Interactions – FoI
: This is a cleanup step where redundant or overlapping interactions get removed from the dataset.

The result of the PLIP Algorithm is a lineup of every interaction for each binding site and ligand[10]. This data has been used as a basis for the machine learning approaches discussed in this thesis.

2.2 Data partitioning

To validate the results of training various machine learning methods the provided data concerning the five targets was split into a training-set as well as a test-set. To achieve a 70/30 train/test split ratio each sample was randomly assigned to one of the two data partitions[24].

In order to validate the machine learning approaches during training 10-fold cross-validation has been applied. For the process of cross-validation the training dataset is split into n equally large subsets. The type of cross-validation implemented in this thesis uses all but one of these partitions to train the classification model and validates the results with the remaining partition. This process is repeated for all possible validation partitions[25].

2.3 Machine-Learning approaches !WIP!

Introduction to the ML Approaches used for the thesis.

2.3.1 K nearest neighbor

2.3.2 Random forest

2.3.3 Neural networks

2.4 Quality metrics

In order to make the results from this thesis comparable to the results from the scoring function introduced in [8] by Micha Birklbauer the same quality metrics have been implemented for this thesis. The following will provide an overview for the used metrics.

2.4.1 Terminology

To calculate the metrics that are mentioned within this chapter the following base terms are necessary:

TP – **T**rue **P**ositives are active samples, which are classified as such

TN – **T**rue **N**egatives are inactive samples, which are classified as such

FP – **F**alse **P**ositives are inactive samples, which are classified as active

FN – **F**alse **N**egatives are active samples, which are classified as inactive

2.4.2 Visual metrics

For better visualization of the four base metrics mentioned in 2.4.1 this thesis displays the resulting data in a confusion matrix. This metric displays distribution of the results over the four base metrics.

In addition to that, the ROC(receiver operating characteristic) curve will also be displayed for the results. The ROC curve is a collection of points in a two-dimensional space, where their location is defined by the FPR 2.4.4 on the x-axis and the TPR($\frac{\#TP}{\#TP+\#FN}$)

on the y-axis. Each point on this line depicts the ratio of FPR to TPR at a certain score cutoff. [26]

2.4.3 Accuracy

Accuracy (ACC) describes which portion of the predicted samples was accurately assigned to the correct class and is defined as follows:

$$\text{ACC} = \frac{\#TP + \#TN}{\#TP + \#TN + \#FP + \#FN}$$

[27]

2.4.4 False positive Rate

False positive Rate (FPR) describes the compounds that were incorrectly classified as active in relation to all inactive compounds dand is defined as follows:

$$\text{FPR} = \frac{\#FP}{\#TN + \#FP}$$

[26]

2.4.5 Area under the curve

Area under the curve (AUC) is a metric which stems from the ROC curve. The integral of the ROC curve is calculated using the scikit-learn package and is always between 0 and 1[26].

2.4.6 Yield of Actives

Yield of actives (Ya) describes the true positive compounds in relation to all as active labeled compounds and is defined as follows:

$$\text{Ya} = \frac{\#TP}{\#TP + \#FP}$$

[28]

2.4.7 Enrichment Factor

The enrichment factor (EF) describes the relation of the truly active compounds among all as active predicted complexes and the relative share of active compounds in the dataset. This metric is defined as follows:

$$\text{EF} = \frac{\frac{\#TP}{\#TP+\#FP}}{\frac{\#TP+\#FN}{\#TP+\#TN+\#FP+\#FN}}$$

[26]

2.4.8 Relative Enrichment Factor

The relative enrichment factor (REF) describes the relation of the EF to the maximum achievable EF. The REF is defined as follows:

$$\text{REF} = \frac{100 * \#TP}{\min(\#TP + \#FP, \#TP + \#FN)}$$

[26]

2.5 Feature engineering

Feature engineering is the process of manipulating the given features within a dataset with the goal of improving the performance of numerous machine learning techniques applied to the manipulated data. The following chapter explains the various methods that have been used for this thesis.

2.5.1 Feature engineering using random forest

Due to the nature of the random forest algorithm, explained in 2.3.2, it can be used effectively to determine the most important features within a dataset. This section introduces the two feature engineering components within this thesis that are based on the random forest algorithm.

Mean Decrease in Impurity (MDI)

The importance of each feature in a random forest is decided by how well a certain feature can divide the samples in to the desired groups. The mean decrease in impurity is a measure designed to indicate this importance. To calculate it the *Gini*-impurity is needed. The Gini-impurity is a measure of how well a dataset can be divided using a certain feature. The Gini-impurity can be calculated at each node of a decision-tree and is ranged from 0 to 0.5. Let k be the number of classes and let p_i be the probability of a sample belonging to the class(i) and the Gini-impurity($Gini(D)$) of the dataset(D) at a certain node within the tree can be defined as follows:

$$Gini(D) = 1 - \sum_{i=1}^{k} \mathrm{p}_i^2$$

[29]

With that in mind the mean decrease in impurity can be calculated with the following steps. At first the initial Gini-impurity needs to be calculated using the formula above with the classes *active* and *inactive*. In a second step it is necessary to calculate the *weighted Gini* after a split by a feature for each feature. This is achieved by multiplying the relative amount of actives with the Gini-impurity of a given feature for an active classification. This is repeated for the inactive component. Those two numbers combined equate the weighted Gini for that feature. The average of the weighted Gini over all features equates to the mean decrease in impurity. Let g_f be the weighted Gini for a

feature(f) and n be the number of features then the mean decrease in impurity(mdi) can be defined as follows:

$$mdi = \frac{1}{n} * \sum_{f=1}^{n} \mathrm{g}_f$$

With this metric the features with larger g_f are deemed the most crucial for classification[30].

In the following, results with the *fe_rf_mdi*-prefix where calculated using this method.

Permutation importance

Permutation importance is a feature engineering technique used to determine the most important features for classification within a tabular dataset. At first a reference score(s) is calculated using a random forest classifier. In the following step a feature column is randomly permutated. After this *corruption* of the source dataset the score is calculated again and compared to the reference score. This step can be repeated K times in order to improve its statistical viability. This process is repeated for all features.

Let j be the feature, K the repetitions per feature and $\mathrm{s}_{k,j}$ the score of each corrupted dataset, and the importance of each feature(i_j) can be calculated as follows:

$$\mathrm{i}_j = s - \frac{1}{K} * \sum_{k=1}^{K} \mathrm{s}_{k,j}$$

If a feature is of greater significance to the model then the score will deviate greater from the reference value[31].

This method is not particularly dependent on the random forest algorithm. The random forest classifier component can be substituted with any other classifier.

In the following, results with the *fe_rf_per*-prefix where calculated using this method.

2.5.2 Physical properties

Feature engineering can also be based on meta-information concerning the provided datasets. For this thesis two methods are proposed to enhance the data by removing possible *noise-features* with the use of additional knowledge concerning the datasets.

Selection of most frequent interactions

To prevent overfitting the forty features(binding-sites) with the most interactions have been selected. By removing the less occurring features the overall performance especially on the validation- and test-runs should improve. Due to the reduction in the amount of features overfitting can be reduced, and the machine learning models are less distracted by “unimportant” features.

In the following, results with the *fe_freq*-prefix where calculated using this method.

Removal of all hydrophobic interactions

Of all, for this thesis considered interactions, hydrophobic interactions are generally the most frequent[32]. Therefore, it is of interest to reduce the overall amount of features

by removing all the hydrophobic interactions from the datasets in order to achieve more granular results.

In the following, results with the *fe_nonhydrop*-prefix where calculated using this method.

2.5.3 Principal component analysis (PCA)

Principal component analysis is a feature engineering method which aims to reduce the noise within a dataset, as well as maximize the amount of variance. PCA works by representing the original dataset as through linear uncorrelated variables or components. This is done in three steps:

1. Restructuring of the data so that the data is represented as a $m \times n$ matrix where m is the number of features and n the number of samples.
2. Subtract off the mean for each feature.
3. Calculation of the principal components using singular value decomposition (SVD).

While the first two steps are quite clear, the third step will be explained in the following.

First the SVD of the dataset needs to be defined.

$$X = U \cdot \Sigma \cdot V^T$$

Where X is the original data matrix, U is the matrix containing the eigenvectors of $X \cdot X^T$, Σ contains the square-roots of the eigenvectors of $X^T \cdot X$ and V contains the eigenvectors of $X^T \cdot X$.

To get the transformed data it is necessary to multiply the U matrix with Σ. The resulting projections are sorted according to variance[33].

In the following, results with the *fe_pca*-prefix where calculated using this method.

2.5.4 Balancing classes

The data used for this thesis is not balanced, as there are more *inactive* samples than *inactives*.

Synthetic minority over-sampling(SMOTE) can be used to balance the provided datasets. The aim of this technique is to synthetically generate samples from the minority class to balance the class distribution. The SMOTE algorithm starts by selecting a sample from the minority class and finding its k nearest neighbors within that class. For each of the selected neighbors the difference to the original sample is calculated. The differences are then scaled with a random factor between 0 and 1. Those scaled values are added to the original sample in order to create new samples. This whole process is repeated for the unbalanced dataset until all classes are equally represented[34].

In the following, results with the *fe_smote*-prefix where calculated using this method.

Chapter 3

Results

The following chapter describes the results from the different machine learning approaches and the applied feature engineering techniques described in Methods.

3.1 Feature Engineering Results for AChE

To evaluate different feature engineering approaches the protein *Acetylcholinesterase* was used. The goal of this evaluation is to determine which feature engineering techniques shall be used on the protein-ligand compounds. It is also of interest, which feature engineering techniques work best with each machine learning approach. The ACC measure is used to score the performance of the feature engineering method. The metric is calculated using the validation data.

Neural network

The following table is the result of applying the neural network on the datasets that where manipulated using feature engineering.

Table 3.1: Feature engineering validation accuracy neural network

Name	Validation Accuracy
baseline_nn	0.7801
fe_smote_nn	0.7801
fe_pca_nn	0.7589
fe_rf_mdi_nn	0.7589
fe_rf_per_nn	0.7518
fe_nonhydrop_nn	0.7376
fe_freq_nn	0.7180

The results state that the neural network approach does not improve greatly when applying the proposed feature engineering methods. The SMOTE method comes close

to the performance of the baseline neural network. Therefore, it will be included for the analysis of the five complexes.

K nearest neighbor

The following table is the result of applying the KNN algorithm on the datasets that where manipulated using feature engineering.

Table 3.2: Feature engineering validation accuracy
k nearest neighbor

Name	Validation Accuracy
fe_rf_mdi_knn	0.7934
fe_rf_per_knn	0.7778
fe_freq_knn	0.7664
fe_nonhydrop_knn	0.7550
fe_pca_knn	0.7550
baseline_knn	0.7437
fe_smote_knn	0.7437

The KNN algorithm benefits greatly from the proposed feature engineering methods. To contrast the baseline KNN performance best, the feature engineering methods using random forest will be evaluated for the protein-ligand complexes, as their performance supersedes the other methods.

Random forest

The following table is the result of applying the random forest algorithm on the datasets that where manipulated using feature engineering.

Table 3.3: Feature engineering validation accuracy
random forest

Name	Validation Accuracy
fe_smote_rf	0.8375
baseline_rf	0.8362
fe_rf_mdi_rf	0.8290
fe_rf_per_rf	0.8221
fe_freq_rf	0.8107
fe_nonhydrop_rf	0.8050
fe_pca_rf	0.8005

The random forest algorithm does not benefit greatly from the proposed feature

engineering methods. Due to the more balanced dataset resulting from the SMOTE method a slight performance boost can be observed. Therefore, the SMOTE algorithm will be applied to the remaining protein-ligand complexes.

Overall performance projections

The following table lists all the feature engineering accuracies for all the machine learning approaches.

Table 3.4: Feature Engineering Validation Accuracy overall

Name	Validation Accuracy
fe_smote_rf	0.8375
baseline_rf	0.8362
fe_rf_mdi_rf	0.8290
fe_rf_per_rf	0.8221
fe_freq_rf	0.8107
fe_nonhydrop_rf	0.8050
fe_pca_rf	0.8005
fe_rf_mdi_knn	0.7934
baseline_nn	0.7801
fe_smote_nn	0.7801
fe_rf_per_knn	0.7778
fe_freq_knn	0.7664
fe_pca_nn	0.7589
fe_rf_mdi_nn	0.7589
fe_nonhydrop_knn	0.7550
fe_pca_knn	0.7550
fe_rf_per_nn	0.7518
baseline_knn	0.7437
fe_smote_knn	0.7437
fe_nonhydrop_nn	0.7376
fe_freq_nn	0.7180

As seen in the table the random forest approaches tend to yield the best result when applied to the validation portions of the datasets. Therefore, this approach is very likely to score better on the test sets as well.

3.2 Performance per Protein-Complex

The following chapter is dedicated to evaluate the different machine learning and feature engineering methods on the target compounds. For each protein the top two approaches are evaluated further.

3.2.1 Acetylcholinesterase

The following table presents the results of the different machine learning algorithms on the various test-sets. The ROC curves for the top two performing configurations can be found at 3.3 and 3.4 respectively. The confusion matrices can be found at 3.1 and 3.2. The scoring functions achieved an accuracy score of 81.06% on the test-set.

Table 3.5: Acetylcholinesterase performance test-set

Name	ACC	FPR	AUC	EF	REF
baseline_rf	0.8106	0.3285	0.7992	1.4161	92.6829
fe_smote_rf	0.8007	0.3358	0.7894	1.4046	91.4634
fe_smote_nn	0.7708	0.2993	0.7650	1.4102	82.9268
baseline_nn	0.7674	0.2920	0.7626	1.4134	81.7073
fe_rf_per_knn	0.7575	0.4307	0.7420	1.3172	91.4634
baseline_knn	0.6844	0.5766	0.6629	1.1966	90.2439
fe_rf_mdi_knn	0.5515	0.4307	0.5530	1.0987	59.8639

Figure 3.1: Baseline random forest confusion matrix

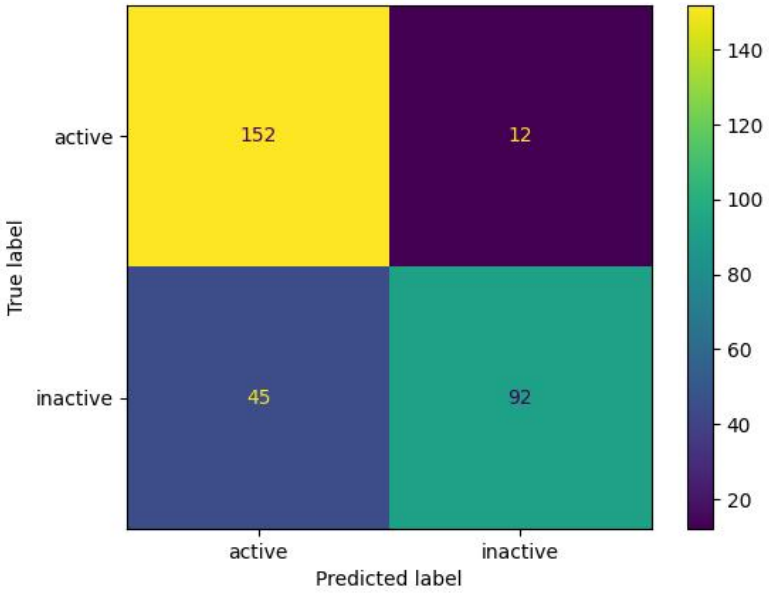

Figure 3.2: SMOTE random forest confusion matrix

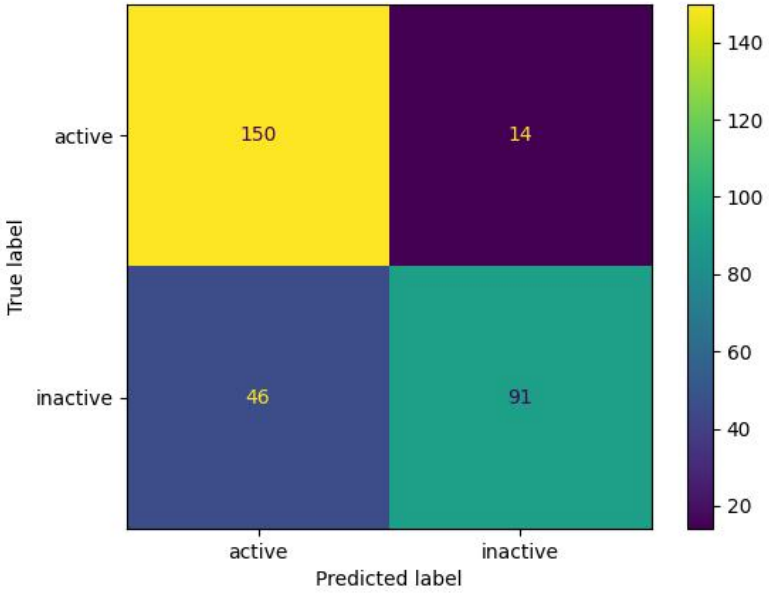

Figure 3.3: Baseline random forest ROC curve

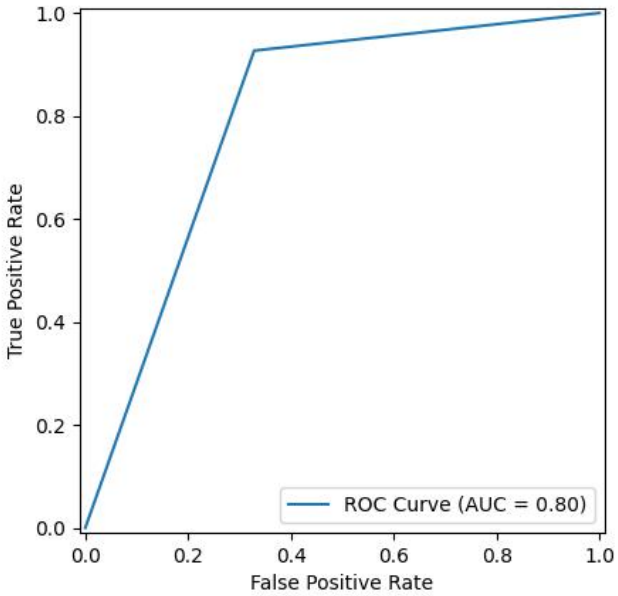

Figure 3.4: SMOTE random forest ROC curve

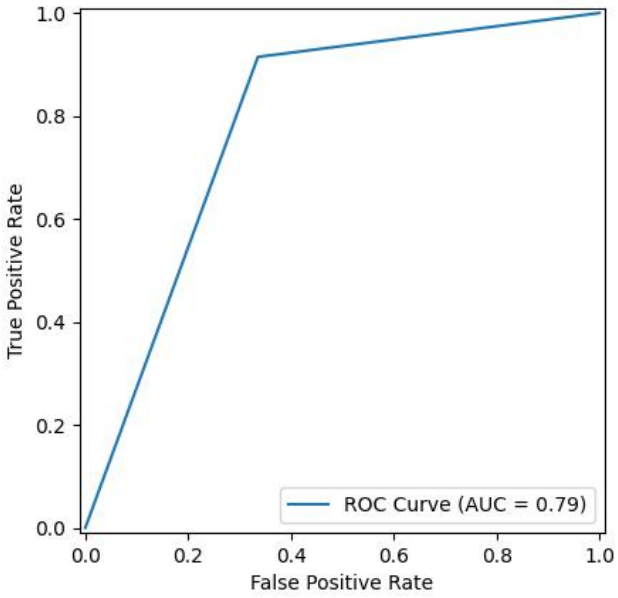

3.2.2 Cyclooxygenase 1

The following table presents the results of the different machine learning algorithms on the various test-sets. The ROC curves for the top two performing configurations can be found at 3.7 and 3.8 respectively. The confusion matrices can be found at 3.5 and 3.6. The scoring functions achieved an accuracy score of 77.24% on the test-set.

Table 3.6: Cyclooxygenase 1 performance test-set

Name	ACC	FPR	AUC	EF	REF
baseline_rf	0.7724	0.0183	0.6344	2.8909	87.0968
fe_smote_rf	0.7628	0.0138	0.6155	2.9362	88.4615
fe_rf_per_knn	0.7019	0.0826	0.5598	1.7044	51.3514
baseline_knn	0.6859	0.1147	0.5544	1.5153	45.6522
baseline_nn	0.6827	0.0872	0.5309	1.4081	42.4242
fe_smote_nn	0.6827	0.1147	0.5490	1.4752	44.4444
fe_rf_mdi_knn	0.6250	0.1835	0.4987	0.9899	29.8246

Figure 3.5: Baseline random forest confusion matrix

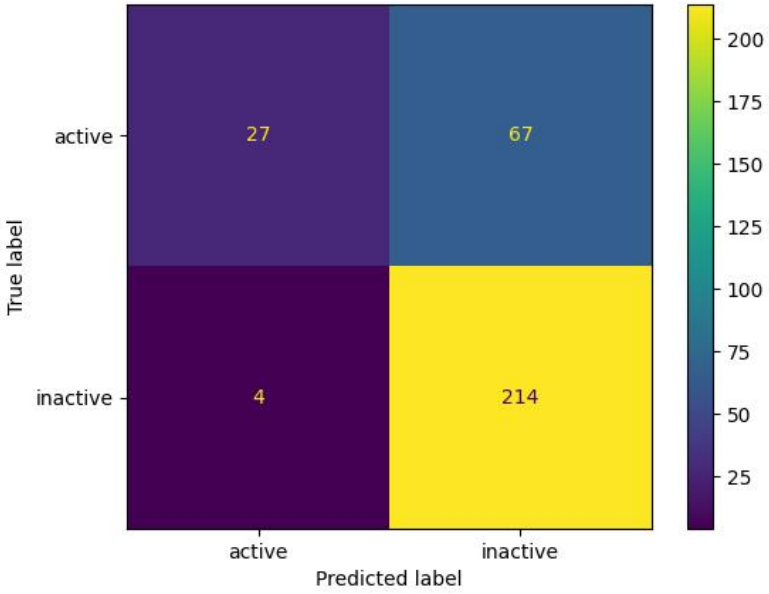

Figure 3.6: SMOTE random forest confusion matrix

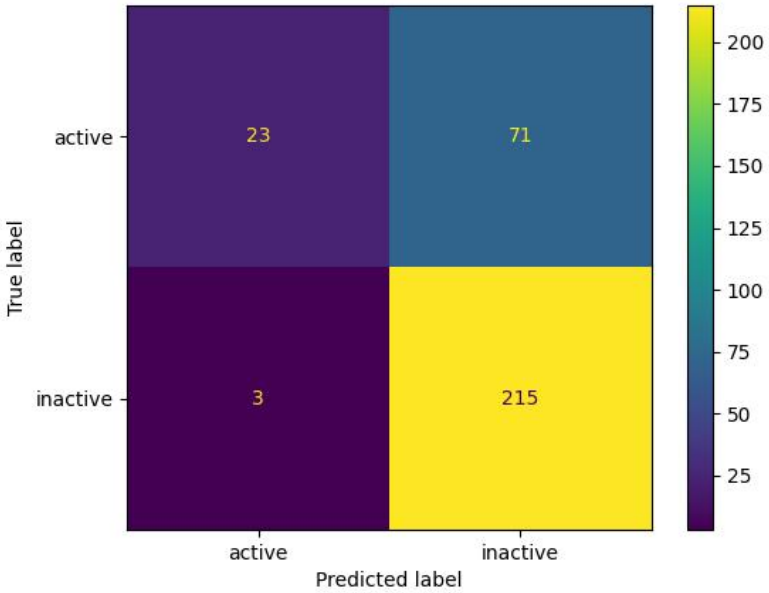

Figure 3.7: Baseline random forest ROC curve

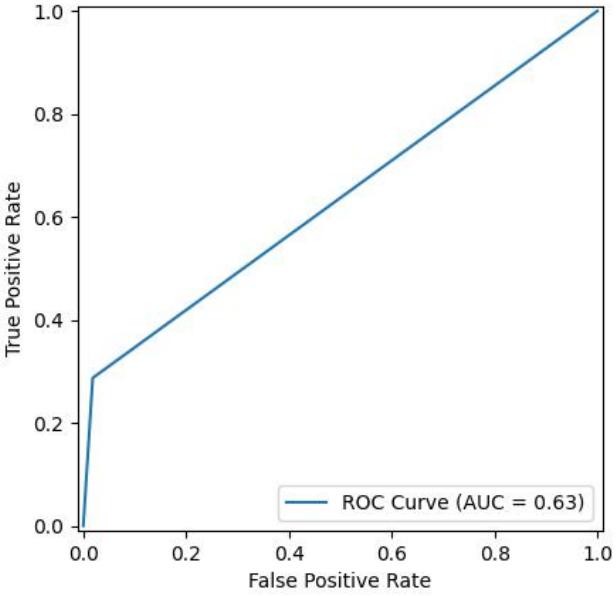

Figure 3.8: SMOTE random forest ROC curve

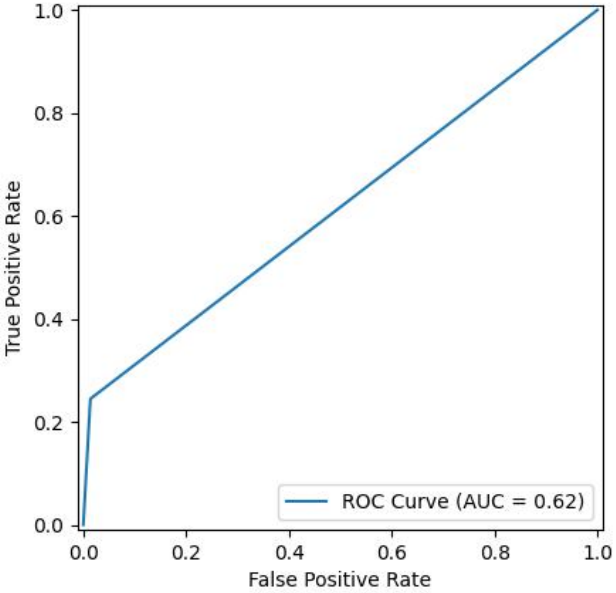

3.2.3 Dipeptidyl peptidase IV

The following table presents the results of the different machine learning algorithms on the various test-sets. The ROC curves for the top two performing configurations can be found at 3.11 and 3.12 respectively. The confusion matrices can be found at 3.9 and 3.10. The scoring functions achieved an accuracy score of 77.21% on the test-set.

Table 3.7: Dipeptidyl peptidase IV performance test-set

Name	ACC	FPR	AUC	EF	REF
baseline_rf	0.7721	0.2041	0.7730	1.5393	79.8387
fe_smote_rf	0.7662	0.2122	0.7670	1.5254	79.1165
fe_rf_per_knn	0.7112	0.3714	0.7082	1.3412	78.7879
baseline_nn	0.6896	0.3347	0.6887	1.3425	71.2121
baseline_knn	0.6896	0.3959	0.6865	1.3046	76.8939
fe_smote_nn	0.6896	0.3306	0.6889	1.3453	70.8333
fe_rf_mdi_knn	0.4892	0.5143	0.4891	0.9791	50.7812

Figure 3.9: Baseline random forest confusion matrix

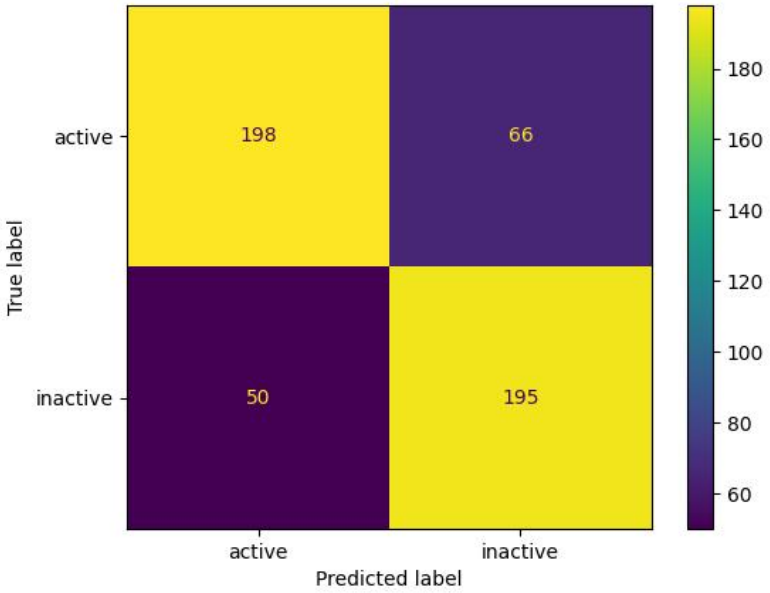

Figure 3.10: SMOTE random forest confusion matrix

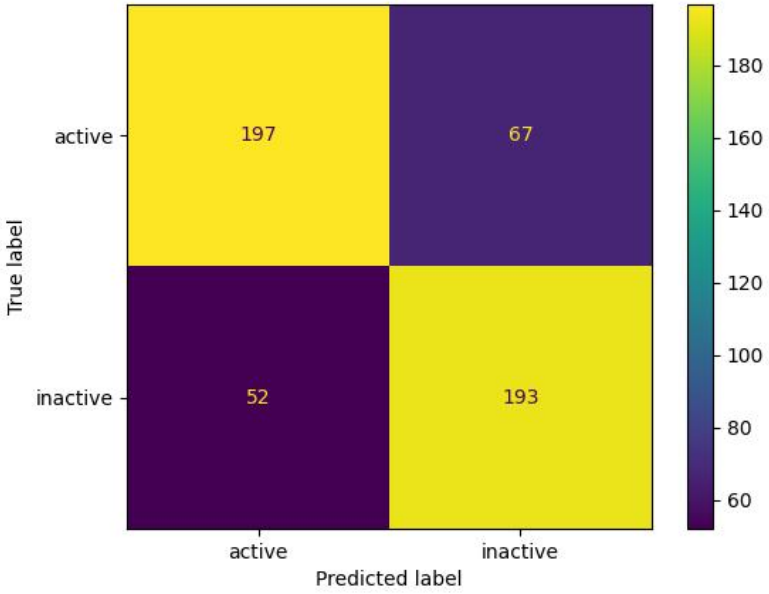

Figure 3.11: Baseline random forest ROC curve

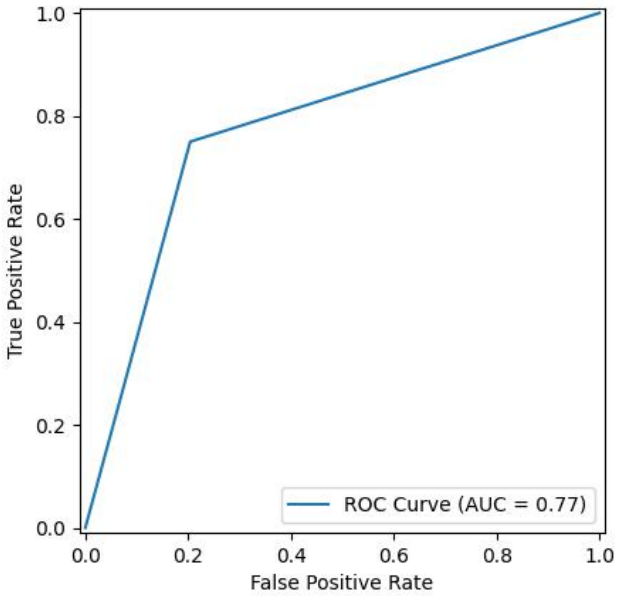

Figure 3.12: SMOTE random forest ROC curve

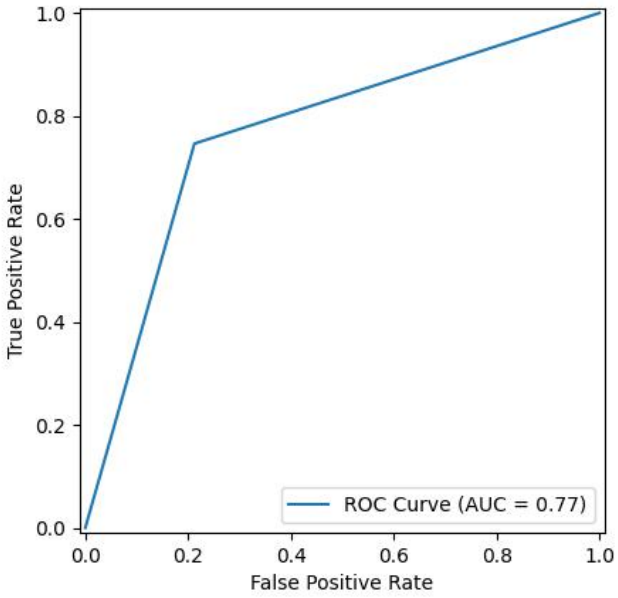

3.2.4 Monoamine oxidase B

The following table presents the results of the different machine learning algorithms on the various test-sets. The ROC curves for the top two performing configurations can be found at 3.15 and 3.16 respectively. The confusion matrices can be found at 3.13 and 3.14. The scoring functions achieved an accuracy score of 75.98% on the test-set.

Table 3.8: Monoamine oxidase B performance test-set

Name	ACC	FPR	AUC	EF	REF
baseline_rf	0.7589	0.1389	0.7181	1.9515	69.6970
fe_rf_per_knn	0.7054	0.1944	0.6653	1.6800	60.0000
fe_smote_rf	0.7054	0.1944	0.6653	1.6800	60.0000
baseline_nn	0.6964	0.1806	0.6472	1.6625	59.3750
baseline_knn	0.6786	0.1667	0.6167	1.6000	57.1429
fe_smote_nn	0.6696	0.2222	0.6264	1.5200	54.2857
fe_rf_mdi_knn	0.5804	0.3333	0.5458	1.1610	42.5000

Figure 3.13: Baseline random forest confusion matrix

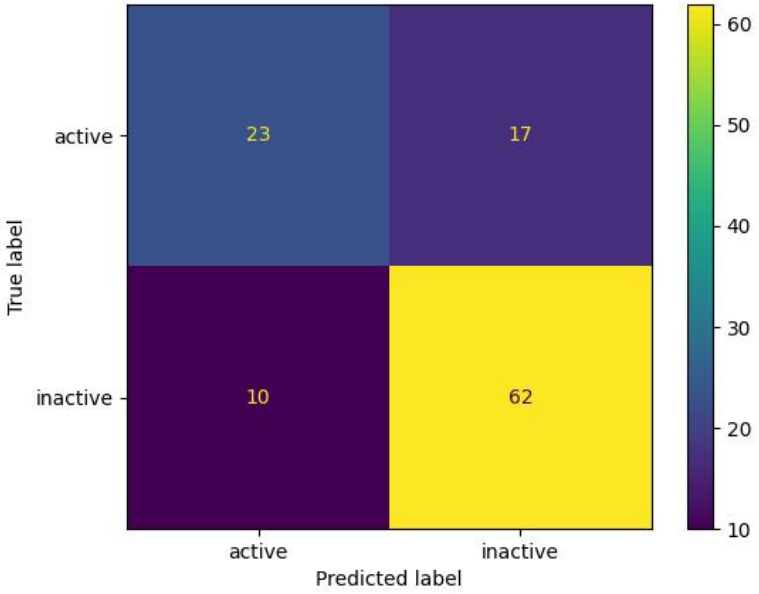

Figure 3.14: Feature engineering permutation importance confusion matrix

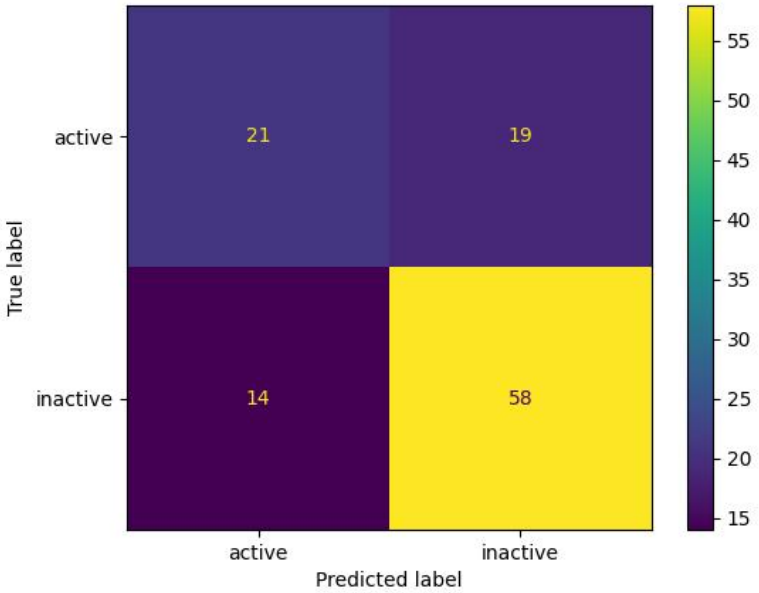

Figure 3.15: Baseline random forest ROC curve

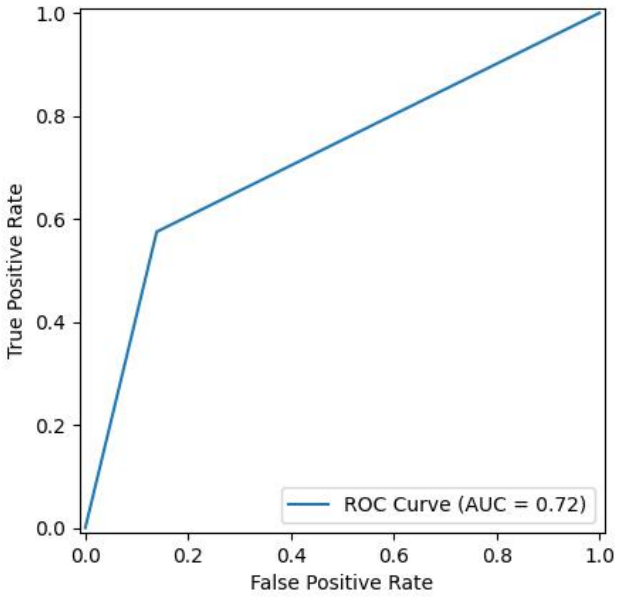

Figure 3.16: Feature engineering permutation importance ROC curve

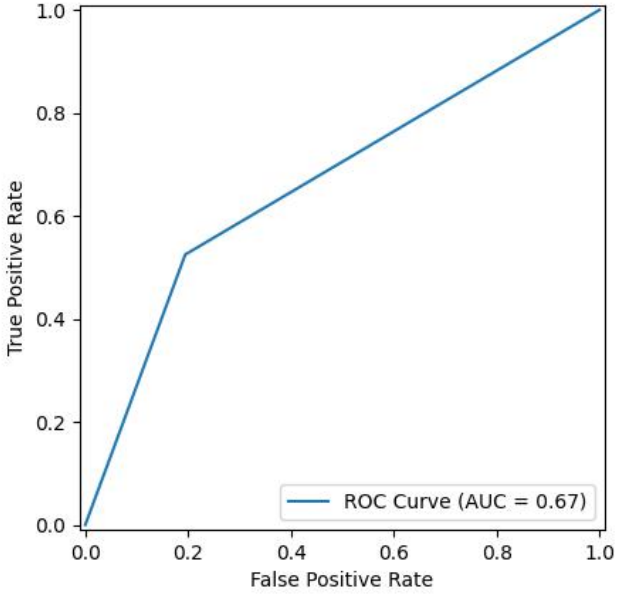

3.2.5 Soluble epoxide hydrolase

The following table presents the results of the different machine learning algorithms on the various test-sets. The ROC curves for the top two performing configurations can be found at 3.19 and 3.20 respectively. The confusion matrices can be found at 3.17 and 3.18. The scoring functions achieved an accuracy score of 80.00% on the test-set.

Table 3.9: Soluble epoxide hydrolase performance test-set

Name	ACC	FPR	AUC	EF	REF
fe_rf_per_knn	0.8000	0.0667	0.6667	2.6667	66.6667
baseline_nn	0.7833	0.0667	0.6333	2.5000	62.5000
baseline_rf	0.7667	0.0000	0.5333	4.0000	100.0000
fe_smote_rf	0.7667	0.0000	0.5333	4.0000	100.0000
baseline_knn	0.7333	0.0222	0.4889	0.0000	0.0000
fe_rf_mdi_knn	0.7000	0.1333	0.5333	1.3333	33.3333
fe_smote_nn	0.7000	0.0889	0.4889	0.8000	20.0000

Figure 3.17: Feature engineering permutation importance confusion matrix

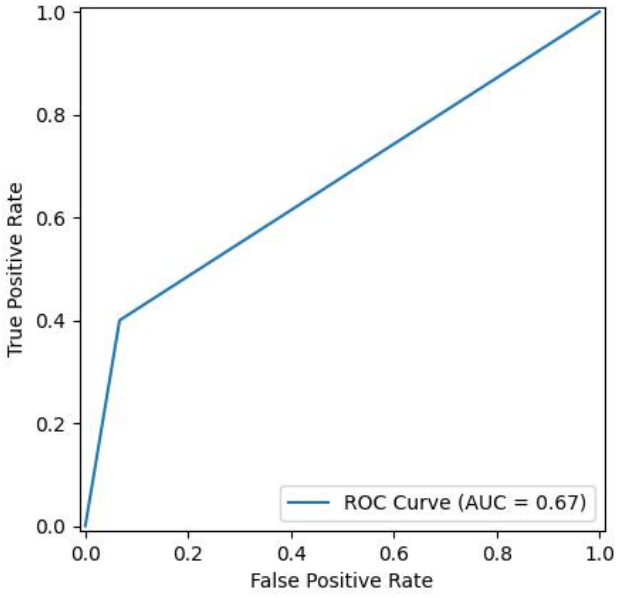

Figure 3.18: Baseline neural network confusion matrix

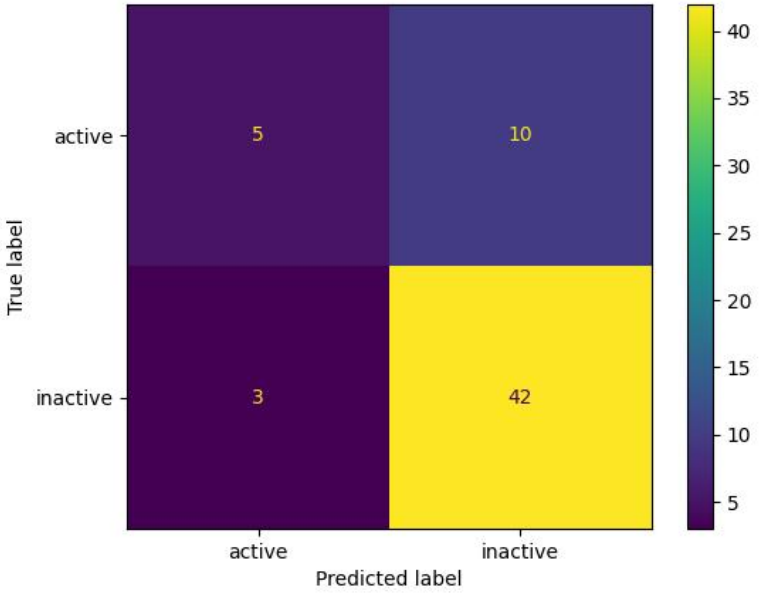

Figure 3.19: Feature engineering permutation importance ROC curve

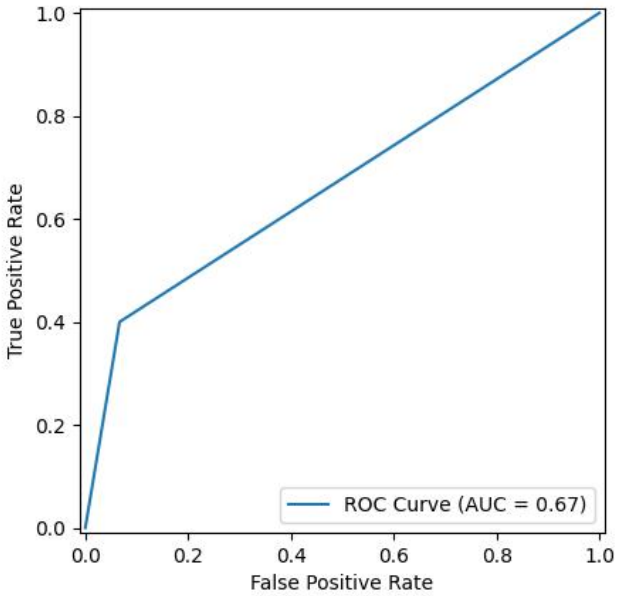

Figure 3.20: Baseline neural network ROC curve

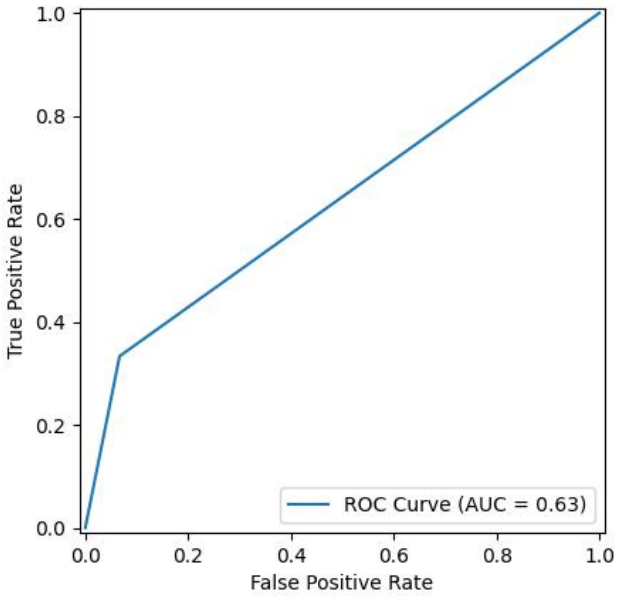

3.3 Performance Overview – Comparing ML-approaches → maybe use median instead of avg ask MICHA

This chapter aims to compare the accumulated results generated in 3.2. To achieve the desired results the best performing version of each machine learning algorithm has been selected for each protein. In the following step the average for each of the machine learning algorithms is calculated. The results of this calculation can be seen in the table below.

Table 3.10: machine learning algorithms comparison

Name	ACC	FPR	AUC	EF	REF
rf	0.7762	0.1380	0.6916	2.3596	85.8631
knn	0.7352	0.2292	0.6684	1.7419	69.6539
nn	0.7246	0.1937	0.6530	1.6647	63.6876

In is obvious that the random forest algorithm outperforms the other algorithms. RF achieves noticeably better performance across all metrics.

Chapter 4

Discussion

4.1 Conclusion

Recap findings of thesis and compare with results from [8] and possible comparable algorithms.

4.2 Improvements and outlook

Explain possible improvements to used technique. Provide general outlook on topic.

Appendix A

Technical Details

Appendix B

Supplementary Materials

List of supplementary data submitted to the degree-granting institution for archival storage (in ZIP format).

B.1 PDF Files

Path: /

thesis.pdf . . . . . Master/Bachelor thesis (complete document)

B.2 Media Files

Path: /media

*.ai, *.pdf . . . . . Adobe Illustrator files
*.jpg, *.png . . . . . raster images
*.mp3 . . . . . audio files
*.mp4 . . . . . video files

B.3 Online Sources (PDF Captures)

Path: /online-sources

Reliquienschrein-Wikipedia.pdf [35]

Appendix C

Questionnaire

Appendix D

LaTeX Source Code

References

Literature

[1] S. Myers and A. Baker. "Drug discovery–an operating model for a new era". eng. *Nature Biotechnology* 19.8 (Aug. 2001), pp. 727–730. DOI: 10.1038/90765 (cit. on p. 1).

[2] Joseph A. DiMasi, Ronald W. Hansen, and Henry G. Grabowski. "The price of innovation: new estimates of drug development costs". eng. *Journal of Health Economics* 22.2 (Mar. 2003), pp. 151–185. DOI: 10.1016/S0167-6296(02)00126-1 (cit. on p. 1).

[3] Lorenz M. Mayr and Peter Fuerst. "The Future of High-Throughput Screening". *SLAS Discovery* 13.6 (July 2008), pp. 443–448. DOI: 10.1177/1087057108319644. (Visited on 02/29/2024) (cit. on p. 1).

[4] Aleix Gimeno et al. "The Light and Dark Sides of Virtual Screening: What Is There to Know?" *International Journal of Molecular Sciences* 20.6 (Mar. 2019), p. 1375. DOI: 10.3390/ijms20061375. (Visited on 02/29/2024) (cit. on pp. 1, 2).

[5] Nataraj S. Pagadala, Khajamohiddin Syed, and Jack Tuszynski. "Software for molecular docking: a review". *Biophysical Reviews* 9.2 (Jan. 2017), pp. 91–102. DOI: 10.1007/s12551-016-0247-1. (Visited on 02/29/2024) (cit. on pp. 1, 2).

[6] A. Lavecchia and C. Di Giovanni. "Virtual screening strategies in drug discovery: a critical review". eng. *Current Medicinal Chemistry* 20.23 (2013), pp. 2839–2860. DOI: 10.2174/09298673113209990001 (cit. on p. 1).

[7] Jin Li, Ailing Fu, and Le Zhang. "An Overview of Scoring Functions Used for Protein–Ligand Interactions in Molecular Docking". en. *Interdisciplinary Sciences: Computational Life Sciences* 11.2 (June 2019), pp. 320–328. DOI: 10.1007/s12539-019-00327-w. (Visited on 02/29/2024) (cit. on p. 2).

[8] Micha Johannes Birklbauer. "Automatic identification of important interactionsand interaction-frequency-based scoring inprotein-ligand complexes". MA thesis. FH Hagenberg, Aug. 31, 2021 (cit. on pp. 2, 6, 7, 28).

[9] Michael M. Mysinger et al. "Directory of Useful Decoys, Enhanced (DUD-E): Better Ligands and Decoys for Better Benchmarking". *Journal of Medicinal Chemistry* 55.14 (July 2012), pp. 6582–6594. DOI: 10.1021/jm300687e. (Visited on 04/30/2024) (cit. on p. 2).

[10] Sebastian Salentin et al. “PLIP: fully automated protein–ligand interaction profiler”. *Nucleic Acids Research* 43.Web Server issue (July 2015), W443–W447. DOI: 10.1093/nar/gkv315. (Visited on 04/23/2024) (cit. on pp. 2, 6).

[11] Balachandran Manavalan and Jooyoung Lee. “SVMQA: support-vector-machine-based protein single-model quality assessment”. eng. *Bioinformatics (Oxford, England)* 33.16 (Aug. 2017), pp. 2496–2503. DOI: 10.1093/bioinformatics/btx222 (cit. on p. 3).

[12] Fatma-Elzahraa Eid, Mahmoud ElHefnawi, and Lenwood S. Heath. “DeNovo: virus-host sequence-based protein–protein interaction prediction”. *Bioinformatics* 32.8 (Apr. 2016), pp. 1144–1150. DOI: 10.1093/bioinformatics/btv737. (Visited on 04/30/2024) (cit. on p. 3).

[13] Bin Li et al. “Development of a Drug-Response Modeling Framework to Identify Cell Line Derived Translational Biomarkers That Can Predict Treatment Outcome to Erlotinib or Sorafenib”. *PLoS ONE* 10.6 (June 2015), e0130700. DOI: 10.1371/journal.pone.0130700. (Visited on 05/01/2024) (cit. on p. 3).

[14] Simon Johansson et al. “AI-assisted synthesis prediction”. *Drug Discovery Today: Technologies*. Artificial Intelligence 32-33 (Dec. 2019), pp. 65–72. DOI: 10.1016/j.ddtec.2020.06.002. (Visited on 05/01/2024) (cit. on p. 3).

[15] Hongming Chen et al. “The rise of deep learning in drug discovery”. eng. *Drug Discovery Today* 23.6 (June 2018), pp. 1241–1250. DOI: 10.1016/j.drudis.2018.01.039 (cit. on p. 3).

[16] Xiangxiang Zeng et al. “Target identification among known drugs by deep learning from heterogeneous networks”. *Chemical Science* 11.7 (), pp. 1775–1797. DOI: 10.1039/c9sc04336e. (Visited on 04/30/2024) (cit. on p. 3).

[17] Oren Z. Kraus, Jimmy Lei Ba, and Brendan J. Frey. “Classifying and segmenting microscopy images with deep multiple instance learning”. *Bioinformatics* 32.12 (June 2016), pp. i52–i59. DOI: 10.1093/bioinformatics/btw252. (Visited on 05/01/2024) (cit. on p. 3).

[18] Connor Morris et al. “MILCDock: Machine Learning Enhanced Consensus Docking for Virtual Screening in Drug Discovery”. *Journal of chemical information and modeling* 62 (Nov. 2022). DOI: 10.1021/acs.jcim.2c00705 (cit. on p. 3).

[19] Anurag Tripathi and U. C. Srivastava. “Acetylcholinesterase :A Versatile Enzyme of Nervous System”. *Annals of Neurosciences* 15.4 (Feb. 2010), pp. 106–111. DOI: 10.5214/95. (Visited on 04/22/2024) (cit. on p. 4).

[20] Carol A. Rouzer and Lawrence J. Marnett. “Cyclooxygenases: structural and functional insights”. *Journal of Lipid Research* 50.Suppl (Apr. 2009), S29–S34. DOI: 10.1194/jlr.R800042-JLR200. (Visited on 04/22/2024) (cit. on p. 4).

[21] Denise M. T. Yu et al. “The dipeptidyl peptidase IV family in cancer and cell biology”. en. *The FEBS Journal* 277.5 (2010), pp. 1126–1144. DOI: 10.1111/j.1742-4658.2009.07526.x. (Visited on 04/22/2024) (cit. on p. 5).

[22] Rona R. Ramsay. “Molecular aspects of monoamine oxidase B”. *Progress in Neuro-Psychopharmacology and Biological Psychiatry* 69 (Aug. 2016), pp. 81–89. DOI: 10.1016/j.pnpbp.2016.02.005. (Visited on 04/22/2024) (cit. on p. 5).

[23] Kara R. Schmelzer et al. “Soluble epoxide hydrolase is a therapeutic target for acute inflammation”. eng. *Proceedings of the National Academy of Sciences of the United States of America* 102.28 (July 2005), pp. 9772–9777. DOI: 10.1073/pnas.0503279102 (cit. on p. 5).

[24] Yun Xu and Royston Goodacre. “On Splitting Training and Validation Set: A Comparative Study of Cross-Validation, Bootstrap and Systematic Sampling for Estimating the Generalization Performance of Supervised Learning”. en. *Journal of Analysis and Testing* 2.3 (July 2018), pp. 249–262. DOI: 10.1007/s41664-018-0068-2. (Visited on 04/21/2024) (cit. on p. 7).

[25] Annette M. Molinaro, Richard Simon, and Ruth M. Pfeiffer. “Prediction error estimation: a comparison of resampling methods”. *Bioinformatics* 21.15 (May 2005), pp. 3301–3307. DOI: 10.1093/bioinformatics/bti499. eprint: https://academic.oup.com/bioinformatics/article-pdf/21/15/3301/50340684/bioinformatics_21_15_3301.pdf (cit. on p. 7).

[26] Julio Cesar Dias Lopes et al. “The power metric: a new statistically robust enrichment-type metric for virtual screening applications with early recovery capability”. *Journal of Cheminformatics* 9.1 (Feb. 2017), p. 7. DOI: 10.1186/s13321-016-0189-4. (Visited on 04/20/2024) (cit. on pp. 8, 9).

[27] Mohammad Hossin and Sulaiman M.N. “A Review on Evaluation Metrics for Data Classification Evaluations”. *International Journal of Data Mining & Knowledge Management Process* 5 (Mar. 2015), pp. 01–11. DOI: 10.5121/ijdkp.2015.5201 (cit. on p. 8).

[28] Deborah Giordano et al. “Drug Design by Pharmacophore and Virtual Screening Approach”. *Pharmaceuticals* 15.5 (May 2022), p. 646. DOI: 10.3390/ph15050646. (Visited on 04/20/2024) (cit. on p. 8).

[29] Fatih Karabiber. *Gini Impurity*. URL: https://www.learndatasci.com/glossary/gini-impurity/ (visited on 05/11/2024) (cit. on p. 9).

[30] Aneesha B. Soman. *Gini Impurity vs Gini Importance vs Mean Decrease Impurity*. en. Oct. 2023. URL: https://medium.com/@aneesha161994/gini-impurity-vs-gini-importance-vs-mean-decrease-impurity-51408bdd0cf1 (visited on 05/11/2024) (cit. on p. 10).

[31] *4.2. Permutation feature importance*. en. URL: https://scikit-learn/stable/modules/permutation_importance.html (visited on 05/10/2024) (cit. on p. 10).

[32] Renato Ferreira de Freitas and Matthieu Schapira. “A systematic analysis of atomic protein–ligand interactions in the PDB”. en. *MedChemComm* 8.10 (Oct. 2017), pp. 1970–1981. DOI: 10.1039/C7MD00381A. (Visited on 05/11/2024) (cit. on p. 10).

[33] Jonathon Shlens. *A Tutorial on Principal Component Analysis*. Tech. rep. arXiv:1404.1100 [cs, stat] type: article. arXiv, Apr. 2014. DOI: 10.48550/arXiv.1404.1100. (Visited on 05/11/2024) (cit. on p. 11).

[34] N. V. Chawla et al. “SMOTE: Synthetic Minority Over-sampling Technique”. *Journal of Artificial Intelligence Research* 16 (June 2002). arXiv:1106.1813 [cs], pp. 321–357. DOI: 10.1613/jair.953. (Visited on 05/11/2024) (cit. on p. 11).

Online sources

[35] *Reliquienschrein*. Aug. 29, 2022. URL: https://de.wikipedia.org/wiki/Reliquienschrein (visited on 02/11/2023).

Check Final Print Size

— Check final print size! —

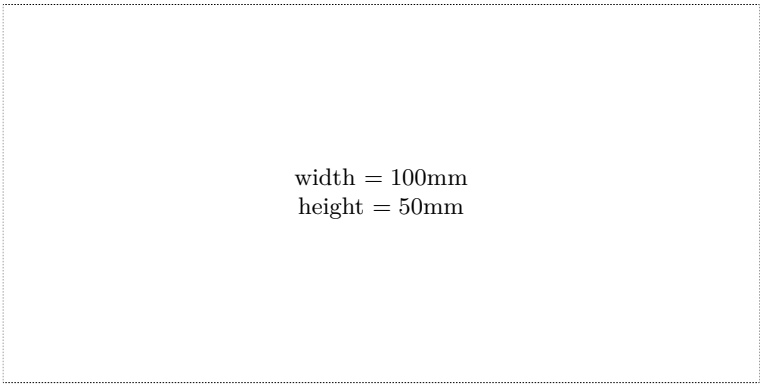

— Remove this page after printing! —